

Evaluation of the Community Land Model 3.5 with Carbon and Nitrogen CYCLES (CLM3.5CN) at a Tibetan GRASSLAND Site

Young-Hee Lee¹, Hee-Jeong Lim¹, Kazuhito Ichii², and Yingnian Li³

¹Kyungpook National University, Daegu, Korea

²Fukushima University, Fukushima, Japan

³Northwest Institute of Plateau Biology, CAS, Qinghai, China

(Manuscript received 18 September 2012; revised 3 March 2013; accepted 3 March 2013)
© The Korean Meteorological Society and Springer 2013

Abstract: The Tibetan plateau plays an important role in energy and carbon cycles by providing an elevated heat source and by storing a large amount of soil carbon due to low temperature. The main vegetation of the plateau is alpine grassland. This study evaluates performance of Community Land Model 3.5 with carbon and nitrogen cycles (CLM3.5CN) over a alpine grassland in the Tibetan plateau in terms of energy and carbon fluxes in conditions of reasonable phenology and initial carbon pool comparable to observations. Comparison between model and observation shows following features. The model captures the magnitude of maximum leaf area index (LAI) but underestimates leaf mass. Net ecosystem exchange (NEE) is significantly underestimated during the growing season and soil temperature is also underestimated throughout a year with higher negative bias in winter than in other seasons. In order to examine the cause of the model deficiencies, we design four sensitivity tests: seasonal mulch; shallow rooting depth; reduction of critical soil moisture to limit the decomposition rate; smaller specific leaf area (SLA). Considering seasonal mulch improves the negative bias of soil temperature during dormant season has little effect on the NEE during the growing season. Underestimation of NEE during the growing season is partly due to underestimated decomposition rate which results from underestimated soil temperature and deep root placement in the soil column. Underestimation of latent heat flux during summer is partly due to use of large SLA in the model. Other deficiencies are also discussed.

Key words: CLM3.5CN, NEE, sensitivity test, Tibetan grassland

1. Introduction

Terrestrial ecosystems play an important role in the global carbon cycle through photosynthesis and ecosystem respiration. Grasslands are one of the most widespread vegetation types covering about 30% of the Earth's surface (Kato *et al.*, 2004). Due to its importance, there have been many observational and modeling studies on temperate and tropical grassland ecosystems (e.g., Kim *et al.*, 1992; Parton *et al.*, 1993). Parton *et al.* (1993) showed that soil carbon and nitrogen levels could be simulated to within 25% of the observed values for a

diverse set of soil including 11 temperate and tropical grasslands by the Century model. Scurlock and Hall (1998) suggested that grasslands may play an important role as a sink of atmospheric carbon although carbon stocks, productivities and turnover times are subject to considerable uncertainty. Many carbon budget studies have been conducted on grassland ecosystems in low elevation areas (e.g., Kim *et al.*, 1992; Sims and Bradford, 2001). Until recently, there have been few studies on carbon fluxes for grassland ecosystems at high elevation areas (e.g., Kato *et al.*, 2004; Gu *et al.*, 2005).

The Qinghai-Tibetan Plateau covers over 2.5×10^6 km² with an average altitude above 4000 m above sea level (Zheng *et al.*, 2000). With its unique topographical feature, the plateau has been considered to play an important role in both energy and carbon cycles. For example, the plateau has been considered as one of the major controlling factors influencing Asian monsoon activity through thermal and mechanical effects (Yanai and Wu, 2006). In addition, the Qinghai-Tibetan plateau is a very sensitive region to climate change with faster temperature rise than in other regions at the same latitude (Liu and Chen, 2000). The main vegetation of the plateau is grassland which area accounts for about 44% of the total grassland area of China (Editorial Board of Vegetation Map of China, 2001). Therefore, revealing energy and carbon budget at the grasslands is important in understanding the regional terrestrial carbon cycle in East Asia.

Recent studies have revealed observational features of energy and carbon dioxide exchange on the plateau. Kato *et al.* (2004) reported that the alpine ecosystem might behave as a sink of atmospheric CO₂ during the growing season and the largest daily CO₂ uptake is less than half of those reported for the lowland grassland and forest at similar latitude. Gu *et al.* (2005) suggested that the phenology of the vegetation and the soil water content were the major factors affecting the energy partitioning in the alpine meadow system. Compared to observational studies on alpine grassland, little attention has been paid to modeling carbon and water vapor exchanges over the Tibetan grassland. Yang *et al.* (2009) offered suggestions on the land surface modeling of the Tibetan plateau such as soil stratification and soil surface resistance focusing on soil temperature and moisture but they did not address carbon cycle

Corresponding Author: Young-Hee Lee, Department of Astronomy and Atmospheric Sciences, Kyungpook National University, Daegu 702-701, Korea.
E-mail: young@knu.ac.kr

issues. Tan *et al.*, (2010) applied the ORCHIDEE global vegetation model to evaluate biomass and soil carbon stocks of Qinghai-Tibetan grasslands. They calibrated the parameterization of ORCHIDEE using multiple time-scale and spatial-scale observations of eddy covariance fluxes, soil temperature and satellite leaf area index and soil organic carbon (SOC) density profile and showed that the calibrated model can successfully capture the seasonal variation of net ecosystem exchange (NEE) as well as the leaf area index (LAI) and SOC spatial distribution. These studies suggest that many land surface models do not simulate the energy exchange and carbon cycle reasonably over the Tibetan plateau with default parameterizations.

The Community Land Model 3.5 with carbon and nitrogen cycles (CLM3.5CN) is a widely used such land surface model. To examine vegetation and climate feedbacks using CLM3.5CN, it is necessary to first assess the performance of the model in simulating carbon and energy fluxes against observations in offline mode. In this study, we evaluate performance of the CLM3.5CN at a grassland site on the Tibetan plateau and suggest possible directions for model improvement through sensitivity tests.

2. Materials and methods

a. Site description and data

The study site (37° 40'N, 101° 20'E, 3430 m a.s.l.) is located in the northeastern part of the Qinghai-Tibetan Plateau. The climate is characterized by highland continental climate with very cold winters. The mean annual air temperature is -1.7°C and mean annual precipitation is about 600 mm. During the growing season, plentiful rainfall occurs and hence soil moisture is ample. The vegetation is typical frigid vegetation of the Northern Qinghai-Tibetan Plateau. The dominant species are *potentilla fruticosa*, *Kobresia humilis*, *Stipa aliena* and *Elymus nutans*.

Measurements of turbulent energy and carbon fluxes were made at 2.2 m above the ground using an eddy covariance system (CSAT3 and LI-7500). The sampling rate was 10 Hz and the averaging time 30 min. We used the CarboEastAsia dataset processed by JapanFlux group (Saigusa *et al.*, 2012). The process includes gap-filling and flux-partitioning for carbon flux data into gross primary productivity (GPP) and ecosystem respiration (RE). The gap-filling and flux partitioning were conducted using the flux analysis tool program (Ueyama *et al.*, 2012). The gap-filling method is based on a combination of a look-up table and non-linear regression methods. The relationships between night-time NEE and air temperature were estimated each day with a 39-days moving window after applying u_* -filtering by fitting to the Lloyd and Taylor equation (Lloyd and Taylor, 1994). Those relationships were used to calculate daytime RE. GPP was calculated as difference between RE and NEE.

Soil temperature at 5-cm depth was measured with a tem-

Table 1. Comparison of annual mean climate data with adjustment with site observation in 2004.

Variable	Climate data	Site observation
Temperature (K)	271	271
Wind speed (m s^{-1})	5.13	1.75
Mixing ratio (mg g^{-1})	3.22	3.80
Total precipitation (mm)	476	516
Shortwave radiation (W m^{-2})	175	199
Pressure (hPa)	640	679
Longwave radiation (W m^{-2})	201	234

perature probe (Model 107, Campbell scientific) and soil water content at 20-cm depth was measured by water content reflectometer (CS616, Campbell Scientific). The measurements of soil temperature and moisture and of the turbulent fluxes were used in comparison with model simulations. The measurements of meteorological and radiation variables were made at 1.2 m and were used as input data for the model in off-line mode for simulation year 2004. The Moderate Resolution Imaging Spectroradiometer (MODIS) LAI was used in comparison with simulated LAI.

To spin up the model, climate data were generated based on the global climate data from 1901 to 2010 with adjustments using meteorological observations at this site (Ichii *et al.*, 2012). The global climate data include the NCEP Reanalysis data (Kalney *et al.*, 1996), the CRU TS3.1 precipitation data (Mitchell *et al.*, 2005), and the GISS solar radiation data (Zhang *et al.*, 2004). Since NCEP reanalysis data are not available for the period of 1901-1947, the reanalysis data for 1948 were used instead. The global climate data are provided at six-hourly. To generate forcing data at model time step, the solar data were fit to the model time step using a diurnal function that depends on the cosine of the solar zenith angle and precipitation were applied evenly across six-hourly period and other variables were linearly interpolated to the model time step. Table 1 shows the comparison between annual mean climate data with adjustment and site observation in 2004. Although wind speed from climate data is much larger than observation, other variables show similar magnitude each other. For nitrogen deposition rate, we used the value of $0.245 \text{ g m}^{-2} \text{ yr}^{-1}$ which was adopted from global data of atmospheric nitrogen deposition in 1993 (Dentener, 2006). Time varying CO_2 concentrations from 1901 to 2004 (Etheridge *et al.*, 1998; Keeling *et al.*, 2009) were used.

b. Model description

CLM3.5CN (Thornton and Zimmermann, 2007; Oleson *et al.*, 2008) simulates bio-geophysical and bio-geochemical processes. The bio-geophysics part calculates hydrology, surface energy fluxes and photosynthesis and the bio-geochemistry part calculates respiration rate, litter and soil carbon and nitrogen states and vegetation phenology. The soil consists of

10 soil layers extending to 3.43 m depth. The one canopy layer is decomposed into two fractions, sunlit and shaded. Soil texture types determine thermal and hydrological properties of the soil. A detailed description on the processes of CLM3.5CN can be found in Oleson *et al.*, (2004), Oleson *et al.*, (2008) and Thornton and Zimmermann (2007). Specific detail on the parameterizations relevant to this study is provided in the following.

(1) Phenology and allocation

The seasonal variation of LAI is modelled using phenology and allocation in the model. The stress-deciduous phenology algorithm handles phenology for vegetation types such as grasses and tropical drought-deciduous trees. These plants can have multiple growing seasons per year. Leaf onset depends on soil water availability and soil temperature. We modified the phenology and allocation schemes to capture the seasonal variation of LAI such as length of the growing season and time of peak LAI at this site. These modifications reduce the effect of unmatched seasonal pattern of LAI on the site simulations, but we do not recommend them for general use in global simulations. Modifications are described in the following.

Onset period lengthens from 15 days to 30 days. When soil temperature is below zero, onset does not occur. The accumulated cold days for leaf offset is calculated when air temperature is less than 5°C instead of 0°C. Alpine grass experiences a dormant period and is known to have short leaf longevity ranging 40 days to 90 days (Eckstein *et al.*, 1999). So here we change leaf longevity from 1 year to 90 days, assume no background litter fall when the number of active days is less than the leaf longevity and allot increased background litter fall in the remaining days instead of using constant background litter fall throughout whole growing season.

A significant portion of the nitrogen is recycled within plants in a process known as translocation which is the withdrawal of nutrients from senescing leaves and subsequent storage within the plants (Bonan, 2008). It is common in trees and grasses also store nutrients in the roots during senescence. Based on this, we changed the proportion of available carbon into growth (F_{cur}) from constant to seasonally varying as follows.

$$\begin{aligned} F_{cur} &= 0.7 & \text{DOY} < 220 \\ F_{cur} &= 0.7 - 0.6(\text{DOY} - 220)/30 & 220 \leq \text{DOY} < 250 \\ F_{cur} &= 0.1 & \text{DOY} \geq 250 \end{aligned}$$

where DOY is day of year.

(2) Nitrogen cycle

Carbon and nitrogen cycles are coupled with each other. Here, we briefly describe the nitrogen cycles and its relationship with carbon cycle in the model. Figure 1 shows schematic of nitrogen cycle including litterfall, decomposition, immobilization, nitrogen deposition, nitrogen fixation, plant uptake and de-nitrification. Nitrogen cycle is coupled with carbon cycle through limiting GPP by available mineral nitrogen

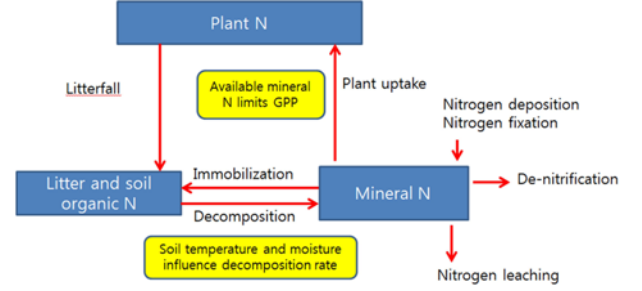


Fig. 1. Schematic of nitrogen cycle in the model.

supply. In model, GPP is first calculated using photosynthesis model and then down-regulated by available mineral nitrogen supply.

Decomposition is major input to mineral nitrogen and decomposition rate is calculated as products of the base decomposition rate and soil temperature and moisture rate scalars. The soil temperature rate scalar is given as

$$f(T) = \sum_{i=1}^{root} \left[\exp \left(308.56 \left\{ \left(\frac{1}{71.02} \right) - \left(\frac{1}{T_{soil}(i) - 227.13} \right) \right\} \right) \right] fr(i) \quad (1)$$

where $T_{soil}(i)$ is temperature at i th soil layer, $fr(i)$ is root fraction of i th soil layer.

The soil moisture rate scalar is given as

$$f(w) = \sum_{i=1}^N \left[\log \left(\frac{\Psi_{min}}{\Psi(i)} \right) \log \left(\frac{\Psi_{min}}{\Psi_{max}} \right) \right] fr(i) \quad \text{for } \Psi(i) > \Psi_{min} \quad (2)$$

where Ψ is soil water potential, Ψ_{min} and Ψ_{max} are minimum and maximum soil water potential, respectively and N is number of soil layer. Ψ_{max} is soil water potential of saturated soil.

(3) Stomatal conductance and leaf photosynthesis

Leaf stomatal conductance, which is needed for the water vapour flux, is coupled to leaf photosynthesis in a manner similar to Collatz *et al.* (1991).

$$g_s = m \frac{A e_s}{c_s e_i} P_{atm} + b \quad (3)$$

where g_s is stomatal conductance ($\mu\text{mol s}^{-1} \text{m}^{-2}$), m is a plant functional type dependent empirical parameter (Collatz *et al.*, 1991), A is leaf photosynthesis ($\mu\text{mol CO}_2 \text{m}^{-2} \text{s}^{-1}$), c_s is the CO_2 concentration at the leaf surface (Pa), e_s is the vapour pressure at the leaf surface (Pa), e_i is the saturation vapour pressure (Pa) inside the leaf at the vegetation temperature, and P_{atm} is the atmospheric pressure (Pa).

Leaf photosynthesis is $A = \min(w_c, w_j, w_e)$ where w_c is RuBP carboxylase limited rate of carboxylation, w_j is the light-limited rate and w_e is export limited rate of carboxylation. Photosynthesis in C3 plants is based on the models of Farquhar *et al.* (1980) and Collatz *et al.* (1991). Maximum carboxylation capacity of Rubisco (V_{cmax}) is formulated as a dynamic quantity that depends on the leaf area based concentration of Rubisco and the enzyme activity (Thornton and Zimmermann, 2007) as

$$V_{cmax} = N_a F_{LNR} \frac{1}{F_{NR}} a_R \quad (4)$$

where N_a is the area-based leaf nitrogen concentration, F_{LNR} is the fraction of leaf nitrogen Rubisco, F_{NR} is the mass ratio of nitrogen in Rubisco molecule to total molecular mass and a_R is the specific activity of Rubisco.

N_a is related to specific leaf area (SLA) and mass-based leaf N content as

$$N_a = \frac{1}{SLA \cdot CN_L} \quad (5)$$

where CN_L is the leaf carbon: nitrogen ratio.

As SLA increases, V_{cmax} decreases and hence A decreases, which leads to decrease of stomatal conductance.

c. Model simulations

We performed a spin-up simulation by cycling through the climatological input from 1901 to 1930. Equilibrium carbon pools were obtained after about 8000 simulation years but the soil carbon amounts (75 kg C m^{-2}) were not comparable to reported values (18 kg C m^{-2} ; Ni, 2002) at a Tibetan alpine meadow. Hence we initialized the model with carbon pool values comparable to the reported. Reasonable soil carbon pools were obtained after 970 simulation years. With the corresponding initial conditions, we performed a transient simulation using climatological data from 1901 to 2003 and variable CO_2 concentration to create initial conditions for simulation year of 2004. For 2004, we used site weather observations as input, to remove any bias from the climatological data. We used the CLM3.5CN with revision to the phenology and allocation (CLM3.5CNp) to focus on the energy and carbon flux simulation under reasonable seasonal variation of LAI.

d. Statistical analysis

Model performance was evaluated using three different statistical indices. The first index was the mean bias error which is the difference between average simulation and average observation.

$$\text{MBE} = \sum_{i=1}^n \frac{P_i - O_i}{n} \quad (6)$$

Where P_i is the simulated data, O_i is the observed data, and n is the number of data.

Positive values of MBE indicate a model overestimation with respect to measured data, while negative values indicate a model underestimation. A second index is root mean squared error (RMSE) between simulated and observed data.

$$\text{RMSE} = \sqrt{\frac{\sum_{i=1}^n (P_i - O_i)^2}{n}} \quad (7)$$

Model results were also evaluated by the index of agreement (d) given by (Willmott, 1982)

$$d = 1 - \frac{\sum_{i=1}^n (P_i - O_i)^2}{\sum_{i=1}^n (|P_i - \bar{P}| + |O_i - \bar{O}|)^2} \quad (8)$$

The index is both a relative and bounded measure which is widely applied in order to make cross-comparisons between model and observation.

3. Results

a. Comparison of model results with observations

(1) LAI and leaf carbon

Daily LAI from the CLM3.5CN and CLM3.5CNp simulations are compared with MODIS LAI (Fig. 2). The magnitude of maximum LAI is captured reasonably well by both simulations. However, CLM3.5CNp appears better at simulating the timing of maximum LAI and the length of the growing season although it still overestimates LAI in the fall. To focus on the simulation of energy and carbon fluxes under reasonable phenology and soil carbon pools, we analyse the simulation results of CLM3.5CNp, hereafter.

Kato *et al.* (2004) reported maximum leaf mass of 347 g m^{-2} in 2001 and 287 g m^{-2} in 2002 at a Tibetan grassland. The leaf mass is dry weight of leaf and the corresponding leaf carbon amounts are 156 gC m^{-2} and 129 gC m^{-2} , respectively. Simulated leaf carbon mass is 46 gC m^{-2} . Although the model captures the maximum LAI, it significantly underestimates leaf mass. This suggests that the value of specific leaf area (SLA) is high in the model.

(2) Energy fluxes and soil temperature and moisture

Daily mean observations were used in evaluating model performance. Table 2 presents performance statistics during total period and growing and dormant seasons. Here, growing

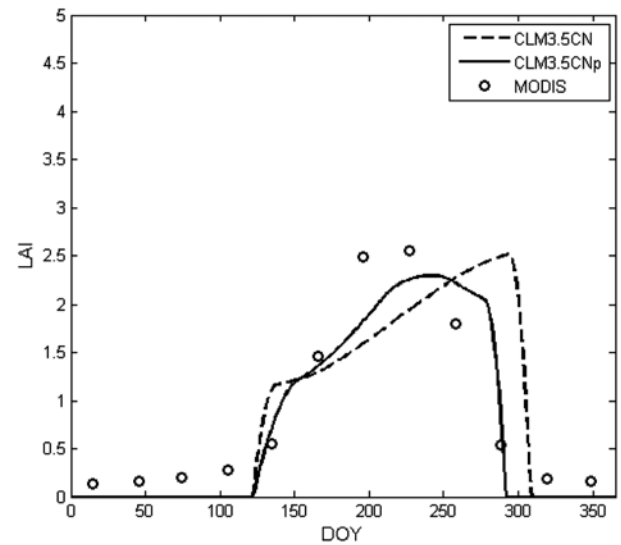


Fig. 2. Comparison of simulated LAI from CLM3.5CN and CLM3.5CNp with MODIS LAI.

Table 2. Statistics of model evaluation for energy fluxes, soil temperature and moisture and carbon fluxes. Growing season is the period from May to October and dormant season is remaining period. MBE, mean bias error; RMSE, root mean square error; d , index of agreement.

	Period	MBE	RMSE	d
Net radiation (W m^{-2})	Total	-22.46	29.01	0.95
	Growing season	-21.07	26.89	0.93
	Dormant sason	-24.11	31.33	0.90
Latent heat flux (W m^{-2})	Total	0.26	16.03	0.94
	Growing season	-0.99	19.99	0.87
	Dormant sason	1.74	9.36	0.87
Sensible heat flux (W m^{-2})	Total	-15.52	27.31	0.66
	Growing season	-11.67	19.07	0.82
	Dormant sason	-20.09	34.63	0.49
Soil temperature (K)	Total	-2.90	3.94	0.94
	Growing season	-2.25	2.83	0.87
	Dormant sason	-3.68	4.94	0.82
Soil water content ($\text{m}^3 \text{m}^{-3}$)	Total	-0.01	0.04	0.95
	Growing season	0.00	0.02	0.81
	Dormant sason	-0.02	0.05	0.84
Net ecosystem exchange ($\text{gC m}^{-2} \text{d}^{-1}$)	Total	0.52	1.35	0.48
	Growing season	0.94	1.80	0.53
	Dormant sason	0.02	0.38	0.63
Gross primary productivity (GPP) ($\text{gC m}^{-2} \text{d}^{-1}$)	Total	-1.62	2.39	0.71
	Growing season	-2.62	3.21	0.63
	Dormant sason	-0.43	0.55	0.41
Ecosystem respi- ration (RE) ($\text{gC m}^{-2} \text{d}^{-1}$)	Total	-1.11	1.56	0.75
	Growing season	-1.69	2.03	0.60
	Dormant sason	-0.42	0.62	0.57

season is defined as the period from May to October and dormant season is remaining period. Figure 3 shows simulated daily mean net radiation, sensible and latent heat fluxes compared to observations. Net radiation is underestimated with a MBE of -22.46 W m^{-2} but its variability is well captured with a d of 0.95. The magnitude of MBE is slightly larger in growing season than in dormant season, which is due to larger radiation amount in growing season than in dormant season.

The model underestimates sensible heat flux with a MBE of -15.52 W m^{-2} during total period and magnitude of MBE is higher during dormant season than during growing season. Some underestimation of sensible heat flux could be due to underestimated net radiation. To examine partitioning of net radiation into sensible and latent heat fluxes, we calculated Bowen ratio using averaged sensible and latent heat fluxes for model and observation. Observed Bowen ratio is 1.11 while simulated one is 0.72. This indicates that model does not simulate well partitioning of net radiation between latent and

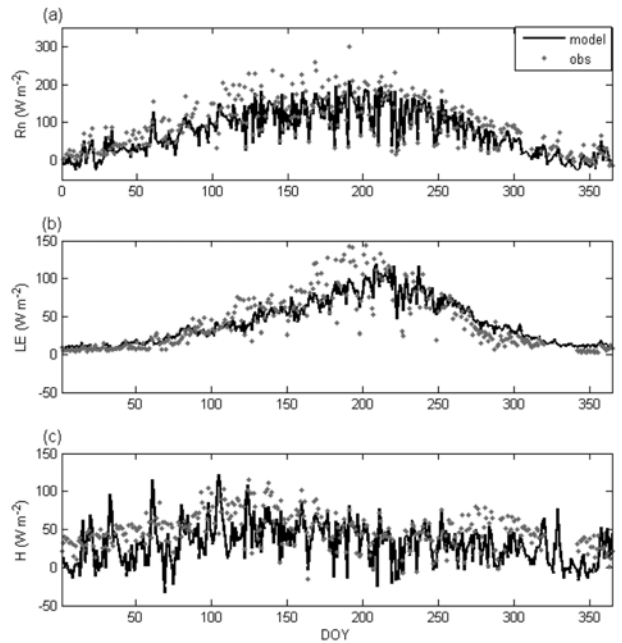


Fig. 3. Comparison of (a) net radiation, (b) latent heat flux and (c) sensible heat flux between model (solid line) and observation (dot).

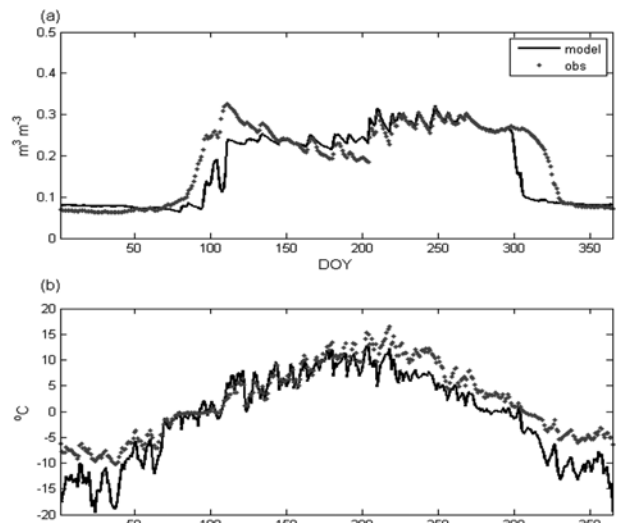


Fig. 4. Comparison of (a) soil water content at 20 cm depth and (b) soil temperature at 5 cm depth between model (solid line) and observation (dot).

sensible heat fluxes. The latent heat flux is well simulated with a MBE of 0.26 W m^{-2} and a d of 0.94. Latent heat flux has strong seasonality which is well captured in model, leading to high correlation between model and observation.

Soil water content is well simulated with no bias during the growing season (Fig. 4a, Table 2). The observed soil water content increases due to melting in spring and then slowly decreases in response to increased evaporation. However, the simulated soil water content shows little decline during growing season. The deficiency in soil moisture variability in CLM3.5 has been also noted by Decker and Zeng (2009), who found a

deficiency in the numerical solution of the soil moisture-based Richards equation using the mass-conservative scheme in CLM. They suggested a revised form of the Richards equation and showed that implementation of the revised scheme resulted in drier soil and increase of soil moisture variability in CLM 3.5. High value of d during total period is due that model captures seasonality of soil water content which is high in summer and low in winter. However, model shows late melting and early freezing of soil water, which may be associated with underestimated soil temperature. Precipitation amount from January to March is 27.5 mm and hence the effect of snow process on soil moisture is not expected to be large.

Soil temperature is underestimated with a MBE of -2.90 K (Fig. 4b). Negative bias is larger in dormant season (-3.68 K) than in growing season (-2.25 K). Underestimated temperature could influence decomposition rate of soil organic carbons through Eq. (1). RMSE has similar magnitude of MBE, indicating that most of errors are due to bias. The values of d for total period is 0.94, indicating that model captures well variability of soil temperature.

(3) Carbon fluxes

The observed carbon fluxes show significant carbon uptake during the growing season while the model shows little uptake during the growing season (Fig. 5a, Table 2). MBE for NEE is 0.52 $\text{gC m}^{-2} \text{d}^{-1}$ for total period and the value of d is 0.48 which is relatively low compared to other variables. Comparison of model results with data-driven estimates shows that GPP is underestimated with a MBE of -1.62 $\text{gC m}^{-2} \text{d}^{-1}$ (Fig. 5b) and RE is also underestimated with a MBE of -1.11 $\text{gC m}^{-2} \text{d}^{-1}$. Positive bias of NEE is due that GPP is more underestimated than RE. In the model, GPP is first calculated using

photosynthesis model and then down-regulated with mineral nitrogen supply from the soil. Comparison of GPP between before and after down-regulation shows that carbon flux is significantly reduced by nitrogen limitation in the model (Fig. 5b). This suggests that nitrogen supply is underestimated in the model, which leads to underestimation of GPP. Nitrogen cycle includes decomposition, plant uptake, nitrogen deposition, and immobilization etc. as explained in section 2b. Nitrogen deposition rate is very low at this site (Dentener, 2006; Lu and Tian, 2007) and hence decomposition is the main supply for mineral nitrogen for plants. Therefore, the underestimated mineral nitrogen results from the underestimated decomposition rate. Decomposition rate depends on soil temperature and moisture as well as carbon pool amounts in the model. Since we used soil carbon pool amounts comparable to the observed, the underestimated decomposition rate may be due to underestimated effect of soil temperature and moisture in rooting depth. And also simple parameterization of nitrogen cycle in the model could lead to uncertainty in mineral nitrogen amount. Note that the simulated GPP before down-regulation is also underestimated, which means that leaf photosynthesis in a given environment is also underestimated in the model. This could be associated with uncertainty of photosynthetic parameter such as V_{cmax} .

b. Sensitivity tests

We investigate the cause of underestimation of carbon uptake and latent heat flux during the growing season with model sensitivity tests. The negative bias of simulated carbon uptake and latent heat flux during the growing season can be due to several reasons. First, underestimated decomposition could result in negative bias of carbon uptake because low decomposition supplies low mineral nitrogen, which severely constrains carbon fluxes. Second, model parameter uncertainty such as SLA and rooting depth could result in negative bias of latent heat flux and carbon flux through the stomatal conductance-

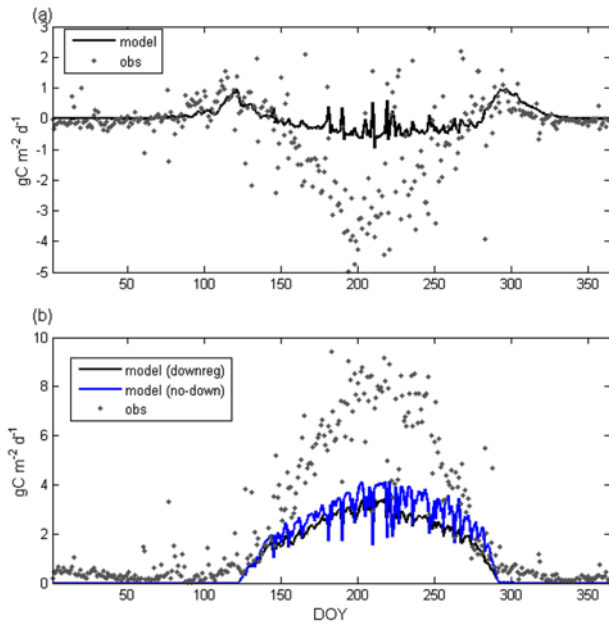


Fig. 5. Comparison of (a) NEE and (b) GPP between model and observation. Model (no-down) and Model (downreg) in (b) indicate GPP before and after considering nitrogen limitation, respectively.

Table 3. Description of sensitivity tests. Seasonal mulch indicates using low thermal conductivity at top two soil layer when DOY <50 or DOY >300 and θ is volumetric water content.

Simulation	Seasonal mulch	Root depth	Critical soil moisture to limit decomposition (θ/θ_{sat})	Specific Leaf area ($\text{m}^2 \text{g}^{-1}$)
Control	No	8 layer (1.38 m)	1	0.05
Test1	Yes	8 layer (1.38 m)	1	0.05
Test2	Yes	6 layer (0.5 m)	1	0.05
Test3	Yes	6 layer (0.5 m)	0.7	0.05
Test4	Yes	6 layer (0.5 m)	0.7	0.02

assimilation relationship (Eqs. (1)-(3)) and the temperature dependence of decomposition. Site specific values of SLA and rooting depth are different from default values in the model. Table 3 lists the sensitivity simulations. The first simulation investigates the effect of seasonal surface litter layer. The other simulations investigate the sensitivity to parameter uncertainty in the model.

(1) Seasonality of surface litter

The model underestimates soil temperature particularly during the dormant season for plants. One possible cause is the lack of a seasonal mulch representation. During the dormant season, dry grass does not decompose due to low temperature and insulates the soil with its low thermal conductivity. In the model, dead standing brown leaf grass is represented as litter with no thermal insulation. Lawrence and Slater (2008) incorporated organic soil into a global climate model but they did not consider the seasonality of litter. Thermal conductivity of peat soil ranges from $0.06 \text{ W m}^{-1} \text{ K}^{-1}$ for dry peat to $0.5 \text{ W m}^{-1} \text{ K}^{-1}$ for saturated one (Arya, 2001). Therefore, for thermal

Table 4. Statistics of model evaluation for soil temperature, energy fluxes and net ecosystem exchange for test 1 during dormant season.

Variable	MBE	RMSE	d
Soil temperature (K)	-1.59	2.29	0.94
Sensible heat flux (W m^{-2})	-16.78	29.94	0.56
Latent heat flux (W m^{-2})	1.97	9.59	0.86
Net ecosystem exchange ($\text{gC m}^{-2} \text{ d}^{-1}$)	0.04	0.39	0.65

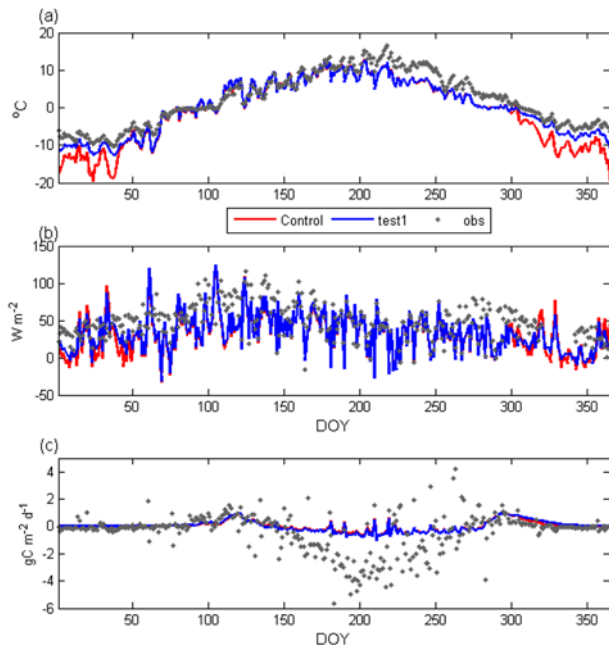


Fig. 6. Comparison of simulated (a) soil temperature moisture at 5 cm depth, (b) sensible heat flux and (c) net ecosystem exchange (NEE) from tests 1 with control run and observation.

conductivity of surface dry litter, we used the value close to that of dry peat. To examine the effect of seasonal litter on the carbon and energy fluxes, we used thermal conductivity of $0.1 \text{ W m}^{-1} \text{ K}^{-1}$ in the top two soil layers when DOY is less than 50 or DOY is greater than 300.

With seasonal mulch, the model shows improvement of soil temperature at 5 cm depth during the period with low thermal conductivity. After that period, simulated soil temperature follows the pattern of the control simulation. Table 4 shows statistics of model evaluation for soil temperature, energy fluxes and net ecosystem exchange for test 1 during dormant season. MBE of soil temperature decreases from -3.68 K to -1.59 K during dormant season. Constant presence of organic layer throughout a year prevents soil from warming rapidly in spring (Lawrence and Slater, 2008). Therefore, underestimation of soil temperature during growing season is not due to neglected surface organic layer during growing season. Use of low soil thermal conductivity leads to low ground heat flux, which results in higher sensible heat flux in winter. Compared to control run, variability of sensible heat flux is reduced in test 1 during dormant season, which is more comparable to observation (Fig. 6a). During dormant season, RMSE decreases from 35 W m^{-2} to 30 W m^{-2} and d increases from 0.49 in control run to 0.56 in test 1. MBE decreases from -20 W m^{-2} to -17 W m^{-2} . The seasonal mulch effect on latent heat flux is small with little change of MBE and RMSE because latent heat flux plays little role in surface energy budget during dormant season.

Although soil temperature is better simulated in test 1, NEE is not affected significantly compared to control run (Fig. 6c and Table 4). Increased winter soil temperature is still far below 0°C and hence little decomposition occurs, which leads to little change to the soil carbon pool.

(2) Sensitivity to model parameters

We examine CLM sensitivity to three parameters related to the decomposition and latent heat flux: Rooting depth; critical soil moisture limiting decomposition rate, Ψ_{max} ; SLA. Rooting depth determines the soil temperature used in the calculation of the decomposition rate (Eq. (1)). At this site, soil thickness is known to be 0.65 m (Kato *et al.*, 2004) and hence the roots of grasses are limited to this soil thickness. In the model, grass roots are distributed in the upper 1.38 m of soil depth. We performed a simulation with rooting depth set to 0.5 m in test 2. In the model, soil moisture limits the decomposition rate when the volumetric water content is below saturation. However, Reichstein *et al.* (2003) identified three phases in the response of soil respiration to soil moisture: (1) When soils are relatively dry, metabolic activity increases strongly with water availability (Howard and Howard, 1993); (2) There is a broad range of near optimum soil water content where changes in soil moisture only have little effect on soil respiration; and (3) above field capacity and toward saturation, oxygen deficiencies inhibit aerobic respiration (Skopp *et al.*, 1990). In test 3, we assume that soil moisture limits the decomposition rate when

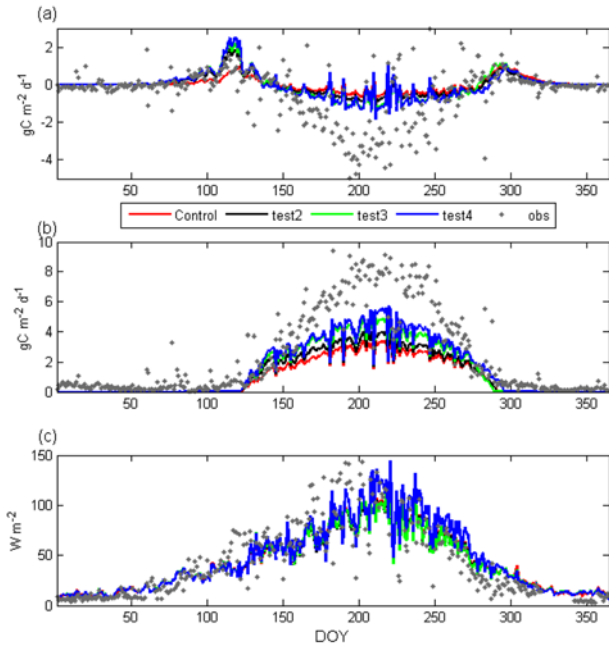


Fig. 7. Comparison of (a) NEE, (b) GPP and (c) latent heat flux from tests 2, 3 and 4 with control run and observation.

Table 5. Statistics of model evaluation for soil temperature, energy fluxes and net ecosystem exchange for test 2, 3, and 4 and control run during summer.

Variable	Simulation	MBE	RMSE	d
Latent heat flux (W m^{-2})	Control	-10.20	24.15	0.71
	Test2	-12.21	25.39	0.69
	Test3	-11.72	24.67	0.70
	Test4	-1.05	22.21	0.79
Sensible heat flux (W m^{-2})	Control	-4.59	11.10	0.92
	Test2	-0.57	10.59	0.93
	Test3	1.50	11.29	0.92
	Test4	-17.54	21.13	0.75
Net ecosystem exchange ($\text{gC m}^{-2} \text{d}^{-1}$)	Control	1.77	2.26	0.47
	Test2	1.59	2.10	0.49
	Test3	1.36	1.89	0.53
	Test4	1.33	1.85	0.54

volumetric water content is less than 70% of saturation and hence Ψ_{\max} in Eq. (2) is calculated as soil water potential of 70% saturation. Test 4 examines the sensitivity of latent heat flux and carbon flux to SLA. Kato *et al.* (2004) reported that SLA of grass at this site is about $0.02 \text{ m}^2 \text{ g}^{-1}$ while default value in the model is $0.05 \text{ m}^2 \text{ g}^{-1}$. Decrease of SLA leads to increases of V_{cmax} which results in increase of stomatal conductance. On the other hand, decrease of SLA also means small leaf area to leaf mass, which leads to reduction of leaf area index in a given GPP. We examined the model sensitivity to site specific value of SLA in test 4.

Table 6. Maximum LAI (LAI_{\max}) and the ratio of maximum LAI to average NEE during summer from observation and model simulations.

	LAI_{\max} ($\text{m}^2 \text{ m}^{-2}$)	$[\text{LAI}_{\max}/\text{NEE}]$ ($\text{m}^2 \text{ m}^{-2} / \text{gC m}^{-2} \text{d}^{-1}$)
Observation	2.5	1.17
Control	2.3	5.72
Test 2	2.4	4.12
Test 3	3.2	3.89
Test 4	1.4	1.62

Figure 7 shows NEE, GPP and latent heat flux from the three sensitivity simulations compared to the control simulation and the observations. The shallow rooting depth increases the decomposition rate due to warmer temperature in the upper soil layers, which increases GPP more than ecosystem respiration, leading to increase of carbon uptake during summer by $0.18 \text{ gC m}^{-2} \text{d}^{-1}$ (Fig. 7a and Table 5). This suggests that spatial variation of soil thickness and rooting depth needs to be considered in global simulation for better simulation of carbon fluxes. Reduction of critical soil moisture also contributes to increase of carbon uptake during the growing season by $0.23 \text{ gC m}^{-2} \text{d}^{-1}$ (Fig. 7a and Table 5, compare test 2 with test 3). However, the increased carbon uptake results in higher maximum LAI than observation (Table 6). Despite increase of LAI, latent heat flux does not show significant increase. This is due that increased transpiration is offset by decreased direct evaporation from the soil.

The slight overestimation of carbon emission in spring may be due to neglecting the dryness of the litter layer. Low moisture significantly limits decomposition rate due to limited metabolic activity (Couteaux *et al.*, 1995). In the model, the decomposition rate of litter and soil carbon is calculated by using one representative soil temperature and moisture of rooting depth. However, moisture conditions between the litter and the top soil layer are quite different due to the high porosity in the litter layer which prevents the capillary rise of liquid water from the soil and hence results in dry litter layer. In the future, a litter layer with separate moisture and temperature should be incorporated in the model and separate consideration for two carbon pool decompositions is required for further improvement.

Comparison between tests 3 and 4 show the effect of changed SLA. Smaller SLA results in significant reduction of maximum LAI but its effect on the carbon uptake is very little because the effect of smaller LAI is offset by larger V_{cmax} . On the other hand, latent heat flux is increased during summer by about 11 W m^{-2} (Fig. 7b and Table 5), indicating that underestimation of the latent heat flux is partly explained by the large SLA in the model. However, sensible heat flux shows large negative bias, which is due that smaller LAI allows more radiation to reach ground, increasing ground heat flux.

Although maximum LAI is lower than observed one in test 4, the ratio of maximum LAI to NEE (1.62) is more comparable to observed one (1.17) compared to ratio of control run

(5.75) (Table 6). The model underestimates mineral nitrogen supply, which leads to underestimation of both NEE and maximum LAI. If more mineral nitrogen were available to the plants, using the observed SLA would result in maximum LAI and NEE comparable with observation.

Although tests 2 and 3 contribute to increase of carbon uptake due to increase of decomposition, the simulated carbon uptake is still lower than observed one (Table 5). One possible cause is underestimated soil temperature in mid-summer which could lead to underestimation of decomposition rate, limiting the nitrogen supply for plants. For better simulation of the carbon flux, the soil physics needs closer examination. And uncertainty of soil carbon pool amount reported at this site may also contribute to negative bias of carbon uptake.

4. Summary

We have evaluated the performance of the CLM3.5CN with modification (CLM3.5CNp) in simulating the energy and carbon fluxes over a Tibetan grassland and identified current problems of the model. Comparison between simulations and observations shows the following features. Maximum LAI is well captured but leaf mass is underestimated. The model underestimates sensible heat flux, which leads to lower Bowen ratio in simulation compared to observation. The simulated soil temperature is lower than observed throughout the year with large cold bias during the dormant season for plants and the simulated soil moisture shows positive bias during growing season and late melting and early freezing due to underestimated soil temperature. The simulated NEE shows little carbon uptake, while observation shows significant carbon uptake during growing season. Comparison between data driven estimated GPP and RE and observations show that both GPP and RE are underestimated. Insufficient mineral nitrogen supply in model limits GPP.

We examine the cause of these model deficiencies by performing 4 sensitivity tests: seasonal mulch; shallow rooting depth; reduction of critical soil moisture to limit the decomposition rate; smaller specific leaf area. Through sensitivity tests, we identify the following causes of model deficiencies and potentials for further improvement. Considering seasonal mulch results in better simulation of the soil temperature during the dormant season but does not significantly change the carbon uptake during the growing season. Some of the deficiencies are due to different model parameter values from observed values at the site. For example, using the observed rooting depth and specific leaf area from this site improves the simulation of carbon uptake and the ratio of maximum LAI to NEE during the growing season. Despite slight improvement in simulation, there are still large negative biases of carbon uptake and soil temperature during growing season. The model error could be due to both model parameter uncertainty and model structural errors. Uncertainty of V_{cmax} and processes of detailed nitrogen cycle and separate consideration of litter in bio-geophysics need to be examined in further study

Acknowledgments. This research was supported by supported by Center for Atmospheric Sciences and Earthquake Research (CATER 2012-7020) and “CarboEastAsia-A3 Foresight Program” of National Research Foundation of Korea.

Edited by: Jimy Dudhia

REFERENCES

- Arya, S. P., 2001: *Introduction to micrometeorology*. Academic press, 420 pp.
- Bonan, G., 2008: *Ecological climatology*. Cambridge University press, 550 pp.
- Collatz, G. J., J. T. Ball, C. Grivet, and J. A. Berry, 1991: Physiological and environmental regulation of stomatal conductance, photosynthesis, and transpiration: A model that includes a laminar boundary layer. *Agric. Forest Meteorol.*, **54**, 107-136.
- Couteaux, M., P. Bottner, and B. Berg, 1995: Litter decomposition, climate and litter quality. *Tree*, **10** (2), 63-66.
- Decker, M., and X. Zeng, 2009: Impact of modified Richards equation on global soil moisture simulation in the community land model (CLM3.5). *J. Adv. Model. Earth Syst.*, **1**, 5.
- Dentener, F. J., 2006: Global maps of atmospheric nitrogen deposition, 1860, 1993, and 2050. Dataset. Available on-line [<http://daac.ornl.gov/>] from Oak Ridge National Laboratory Distributed Active Archive Center, Oak Ridge, Tennessee, U.S.A.
- Eckstein, R. L., P. S. Karlsson, and M. Weih, 1999: Leaf life span and nutrient resorption as determinants of plant nutrient conservation in temperate-Arctic region. *New Phytol.*, **143**, 177-189, doi:10.1046/j.1469-8137.1999.00429.x.
- Editorial Board of Vegetation Map of China, Chinese Academy of Sciences, 2001: *Vegetation Atlas of China*, Science press, Beijing.
- Etheridge, D. M., and Coauthors, 1998: Historical CO₂ records from the Law Dome DE08, DE08-2, and DSS ice cores. In trends: A compendium of data on global change. Carbon Dioxide Information Analysis Center, Oak Ridge National Laboratory, U. S. Department of Energy, Oak Ridge, Tenn, U. S. A.
- Farquhar, G. D., S. von Caemmerer, and J. A. Berry, 1980: A biochemical model of photosynthetic CO₂ assimilation in leaves of C3 species. *Planta*, **149**, 78-90.
- Gu, S., and Coauthors, 2005: Short-term variation of CO₂ flux in relation to environmental controls in an alpine meadow on the Qinghai-Tibetan Plateau. *J. Geophys. Res.*, **108** (D21), 4670, doi:10.1029/2003JD003584.
- Howard, D. M., and P. J. A. Howard, 1993: Relationships between CO₂ evolution, moisture content and temperature for a range of soil types. *Soil Biol. Biochem.*, **25**, 1537-1546.
- Ichii, K., and Coauthors, 2012: Site-level model-data synthesis of terrestrial carbon cycle in the CarboEastAsia eddy-covariance observation network: Toward future modeling efforts. *J. Forest Res.*, (in press), doi:10.1007/s10310-012-0367-9.
- Kato, T., and Coauthors, 2004: Carbon dioxide exchange between the atmosphere and an alpine meadow ecosystem on the Qinghai-Tibetan Plateau, China. *Agric. Forest Meteorol.*, **124**, 121-134.
- Kalney, E., and Coauthors, 1996: The NCEP/NCAR 40-year reanalysis project. *Bull. Amer. Meteor. Soc.*, **77**, 437-471.
- Keeling, R. F., S. C. Piper, A. F. Bollenbacher and J. S. Walker, 2009: Atmospheric CO₂ records from sites in the SIO air sampling network. In trends: A compendium of data on global change. Carbon dioxide information analysis center, Oak Ridge national Laboratory, U. S. Department of Energy, Oak Ridge, Tenn., U.S.A. doi:10.3334/CDIAC/atg.035.
- Kim, J., S. B. Verma, and R. J. Clement, 1992: Carbon dioxide budget in a

- temperate grassland ecosystem. *J. Geophys. Res.*, **97**, 6057-6063.
- Lawrence, D. M., and A. G. Slater, 2008: Incorporating organic soil into a global climate model. *Climate Dyn.*, **30**, 145-160.
- Liu, X., and B. Chen, 2000: Climate warming in the Tibetan Plateau during recent decades. *Int. J. Climatol.*, **20**, 1729-1742, doi:10.1002/1097-0088.
- Lloyd, J., and J. A. Taylor, 1994: On the temperature dependence of soil respiration. *Functional Ecology*, **8**, 315-323.
- Lu, C. and H. Tian, 2007: Spatial and temporal patterns of nitrogen deposition in China: Synthesis of observational data. *J. Geophys. Res.*, **112**, D22S05, doi: 10.1029/2006JD007990.
- Mitchell, T. D., and P. D. Jones, 2005: An improved method of constructing a database of monthly climate observations and associated high-resolution grids. *Int. J. Climatol.*, **25**, 693-712.
- Ni, J., 2002: Carbon storage in grasslands of China. *J. Arid Environ.*, **50**, 205-218.
- Oleson, K., and Coauthors, 2004: Technical Description of the Community Land Model (CLM). , NCAR Technical Note NCAR/TN-461+STR, 173 pp.
- _____, and Coauthors, 2008: Improvements to the Community land model and their impact on the hydrological cycle. *J. Geophys. Res.*, **113**, G01021, doi:10.1029/2007JG000563.
- Parton, W. J., and Coauthors, 1993: Observations and modelling of biomass and soil organic matter dynamics for the grassland biome worldwide. *Global Biogeochem. Cycles*, **7**, 785-809.
- Reichstein, M., and Coauthors, 2003: Modeling temporal and large-scale spatial variability of soil respiration from soil water availability, temperature and vegetation productivity indices. *Global Biogeochem. Cycles*, **17(4)**, 1104, doi:10.1029/2003GB002035.
- Saigusa, N., and Coauthors, 2012: CarboEastAsia and uncertainties in the CO₂ budget caused by different data processing. *J. Forest Res.*, (in press), doi:10.1007/s10310-012-0378-6.
- Sims, P., and J. A. Bradford, 2001: Carbon dioxide fluxes in a southern plains prairie. *Agric. Forest Meteorol.*, **109**, 117-134.
- Scurlock, J. M. O., and D. O. Hall, 1998: The global carbon sink: a grassland perspective. *Global Change Biol.*, **4**, 229-233.
- Skopp, J., M. D. Jawson, and J. W. Doran, 1990: Steady-state aerobic microbial activity as a function of soil water content. *Soil Sci. Soc. Amer. J.*, **54**, 1619-1625.
- Tan, K., and Coauthors, 2010: Application of the ORCHIDEE global vegetation model to evaluate biomass and soil carbon stocks of Qinghai-Tibetan grasslands. *Global Biogeochem. Cycles*, **24**, GB1013, doi: 10.1029/2009GB003530.
- Thornton, P. E., and N. E. Zimmermann, 2007: An improved canopy integration scheme for a land surface model with prognostic canopy structure. *J. Climate*, **20**, 3902-3923.
- Ueyema, M., and Coauthors, 2012: Influences of various calculation options on heat, water and carbon fluxes determined by open- and closed-path eddy covariance methods. *Tellus*, **64B**: doi:10.3402/Tellusb.v64i0.19048.
- Willmott, C. J., 1982: Some comments on the evaluation of model performance. *Bull. Amer. Meteor. Soc.*, **63(11)**, 1309-1313.
- Yanai, M., and G. X. Wu, 2006: Effects of the Tibetan Plateau. *The Asian Monsoon*, edited by B. Wang, Springer, 513-549.
- Yang, K., Y.-Y. Chen, and J. Qin, 2009: Some practical notes on the land surface modeling in the Tibetan Plateau. *Hydrol. Earth Syst. Sci.*, **13**, 687-701.
- Zhang, Y., W. B. Rossow, A. A. Lacis, V. Oinas, M. I. Mishchenko, 2004: Calculation of radiative fluxes from the surface to top of atmosphere based on ISCCP and other global data sets: Refinements of the radiative transfer model and the input data. *J. Geophys. Res.*, **109**, D19105, doi:10.1029/3004JD004457.
- Zheng, D., Q. S. Zhang, and S. H. Wu, 2000: *Mountain Geocology and Sustainable Development of the Tibetan Plateau*. Kluwer Academic Publishers, Dordrecht, The Netherlands, 393 pp.